Volume 9
Number 5
May 2024
Pages 977–1264

Reaction Chemistry & Engineering

Linking fundamental chemistry and engineering to create scalable, efficient processes

rsc.li/reaction-engineering

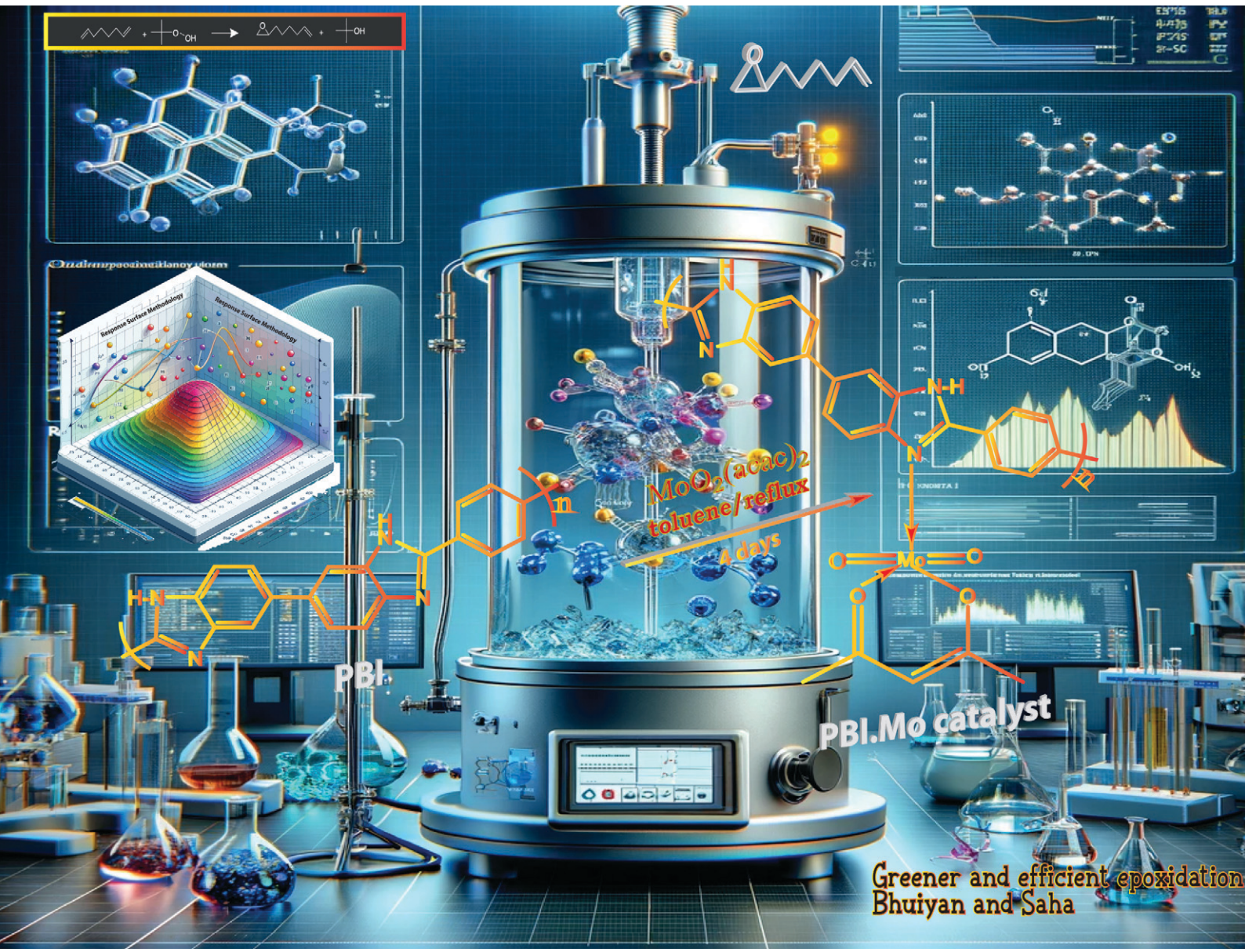

ISSN 2058-9883

ROYAL SOCIETY OF CHEMISTRY

PAPER

Md Masud Rana Bhuiyan and Basudeb Saha
Optimisation of greener and more efficient 1,7-octadiene epoxidation catalysed by a polymer-supported Mo(VI) complex *via* response surface methodology

Reaction Chemistry & Engineering

ROYAL SOCIETY OF CHEMISTRY

PAPER

View Article Online
View Journal | View Issue

Cite this: *React. Chem. Eng.*, 2024, **9**, 1036

Optimisation of greener and more efficient 1,7-octadiene epoxidation catalysed by a polymer-supported Mo(VI) complex *via* response surface methodology

Md Masud Rana Bhuiyan and Basudeb Saha *

In this study, a greener and more efficient alkene epoxidation process has been developed using a heterogeneous polybenzimidazole supported Mo(VI) catalyst and *tert*-butyl hydroperoxide (TBHP) as an oxidising reagent. Polybenzimidazole supported Mo(VI) complex, *i.e.*, PBI·Mo has been prepared, characterised, and evaluated successfully. Batch epoxidation experiments have been carried out in a jacketed stirred batch reactor to evaluate the catalytic activity and stability of PBI·Mo catalyst for the epoxidation of 1,7-octadiene. The suitability and efficiency of the catalyst have been compared by studying the effect of four independent factors such as reaction temperature, the feed mole ratio of 1,7-octadiene to TBHP, catalyst loading, and reaction time on the yield of 1,2-epoxy-7-octene for optimisation of reaction conditions. Response surface methodology (RSM) using Box–Behnken design (BBD) was employed for designing experimental runs and studying the interaction effect of different variables on the reaction response. A quadratic regression model has been developed representing an empirical relationship between reaction variables and response. To determine the adequacy of the predicted model, numerous statistical validation techniques including analysis of variance (ANOVA) have been applied at a 95% confidence level. The numerical optimisation technique concluded that the maximum yield that can be reached is 66.22% at a feed molar ratio of 7.97 : 1, reaction temperature of 347 K, 0.417 mol% catalyst loading, and reaction time of 218 min. The predicted optimal conditions have been validated experimentally with a 1.92% relative error.

Received 1st September 2023,
Accepted 20th February 2024

DOI: 10.1039/d3re00461a

rsc.li/reaction-engineering

Introduction

Alkene epoxidation has been established as an important process for chemical synthesis because it enables the direct oxidation of two adjacent carbon atoms from an alkene using catalysts made of transition metal complexes and oxidising agents such hydroperoxides, peracids, or molecular oxygen in the presence of oxidising reagents.[1–3] The three-membered ring unit of epoxide shows straightforward elaboration to useful new functionality by opening the epoxide ring.[4] The resultant epoxide acts as a raw material or intermediate that can be transformed into many useful substances such as plasticizers, perfumes, and epoxy resins.[5] The importance of epoxides has made the alkene epoxidation reaction one of the most widely studied reactions in organic chemistry.[6] In the fine chemical industries, the conventional epoxidation method represents stoichiometric peracids *e.g.*, peracetic acid and *m*-chloroperbenzoic acid or chlorohydrin as oxidising agents in liquid phase batch reactions.[7,8] This process has the drawback that using these reagents is not environmentally friendly because peracids produce an equivalent amount of acid waste while chlorohydrin produces chlorinated by-products.[8] Additionally, there are security concerns related to the handling and storage of peracid.[9] The Halcon process, which is catalysed by homogeneous Mo(VI) or heterogeneous Ti(IV) supported on SiO_2, is another important liquid phase epoxidation.[10] Due to corrosion and deposition on the reactor, as well as significant requirements in terms of work-up, product isolation, and purification techniques, homogeneous catalysed epoxidation methods are not economically viable for industrial applications.[11] There is a great need for safer epoxidation processes that generate little waste. Because of this, efforts have been made to develop more environmentally friendly and effective epoxidation processes that use a heterogeneous catalyst and a safe oxidant.

Various attempts have been made to find acceptable heterogeneous catalysts for epoxidation by immobilisation of catalytically active metal species on organic or inorganic materials, such as silica,[12,13] zeolites,[14,15] alumina,[16,17] ion-exchange resins,[18,19] polymers, and metal–organic frameworks.[20] However, polymer-supported heterogeneous

School of Engineering, Lancaster University, Lancaster LA1 4YW, UK.
E-mail: b.saha@lancaster.ac.uk

catalysts have been successfully used for the synthesis of epoxides in recent years in the presence of alkyl hydroperoxide as an oxidant and have shown high catalytic activity and product selectivity.[21] Due to polymers' stability, inertness, nontoxicity, and insoluble nature, polymers have attracted attention as potential substrates for catalysts. However, despite numerous published works on polymer-supported Mo(VI) catalysts in the epoxidation of different alkene substrates, there appears to be no report yet on the epoxidation of 1,7-octadiene with *tert*-butyl hydroperoxide as an oxidising reagent in the presence of polymer-supported Mo(VI) catalyst.

In this process, an efficient and selective polybenzimidazole supported molybdenum(VI) complex (PBI·Mo) has been used as a catalyst for the batch epoxidation of 1,7-octadiene. This system is free of solvents and uses the environmentally friendly TBHP as an oxidant. Experiments have been carried out to study the effect of different parameters including reaction temperature, feed molar ratio of alkene to TBHP, and catalyst loading on the yield of 1,2-epoxy-7-octene to optimize the reaction conditions in a classical batch reactor. A quadratic regression model has been developed representing an empirical relationship between reaction variables and response. Response surface methodology (RSM) using Box–Behnken design (BBD) was employed for designing experimental runs and studying the interaction effect of different variables on the reaction response. This study presents the optimization of 1,7-octadiene epoxidation using TBHP as an oxidant and polymer-supported Mo(VI) complex as a catalyst in a batch reactor.

Materials and methods

Materials

All chemicals used during catalyst preparation were purchased from Sigma-Aldrich Co Ltd. and gas chromatography (GC) was used to verify the purity of the chemicals. Microporous polybenzimidazole (PBI) resin beads were supplied by Celanese Corporation, USA. The preparation of polybenzimidazole supported Mo(VI) complex, *i.e.*, PBI·Mo catalyst was carried out using sodium hydroxide (purum p.a. ≥98%), deionised water, acetone, molybdenyl acetylacetonate ($MoO_2(acac)_2$) (99%), and toluene (anhydrous, 99.8%). Reactants involved in this study were 1,7-octadiene (97%) and *tert*-butyl hydroperoxide (TBHP) solution in water (70% (w/w)). The water content of TBHP was removed by the Dean–Stark apparatus from the toluene solution and the concentration of the resulting TBHP solution was determined by iodometric titration. The concentration of TBHP in toluene was found to be 3.57 mol L^{-1}. The quantification of samples collected from the reactor was carried out using the internal standard method in the GC and iso-octane (anhydrous, 99.8%) was used as an internal standard.

Preparation and characterisation of polymer-supported Mo(VI) catalyst

PBI has a high degree of thermal stability as PBI can be heated at high temperatures, and it never melts or burns.[22] These characteristics make PBI resin ideal for a range of uses, including ion-exchange, separations, purifications, and support for polymer-supported catalysts.[9] NaOH solution (1 M) was used to stir wet polybenzimidazole (PBI) resin beads. The polymer beads were then washed with deionised water; then acetone was used to wash the polymer beads. Thereafter, the beads were collected and dried under a vacuum at 40 °C. The treated PBI resin was refluxed with excess $MoO_2(acac)_2$ in anhydrous toluene for a period of 4 days. The PBI·Mo catalyst particles were separated by filtration at the end of the reaction and excess $MoO_2(acac)_2$ was removed by exhaustive extraction with acetone. The green colour disappeared by washing upon repeated introduction of fresh solvent until the solution remained colourless. It was observed that molybdenum in the produced catalysts was uniformly distributed throughout the polymer. The synthesis of polybenzimidazole supported Mo(VI) (PBI·Mo) catalyst is shown in Fig. 1. Malvern Mastersizer was used to determine the particle size distribution of PBI·Mo catalyst. Brunauer–Emmett–Teller (BET) surface area, pore volume, and pore diameter were determined by nitrogen adsorption and desorption method using Micromeritics Gemini VII. The molybdenum content of the prepared catalysts was analysed using a PerkinElmer NexION 350D spectrophotometer. The properties of the prepared PBI·Mo catalyst are given in Table 1.

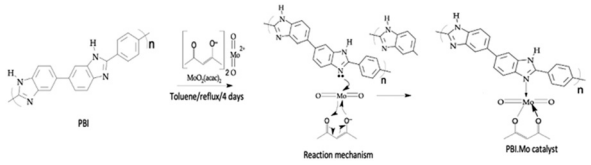

Fig. 1 Reaction mechanism for the synthesis of polybenzimidazole supported Mo(VI) (PBI·Mo) complex.

Experimental design

Response surface methodology (RSM) is a collection of statistical and mathematical techniques for designing, modifying, and optimising processes. It is a useful tool for examining the interactions between factors and quantitatively illustrating how certain parameters affect measured responses.[23] RSM was designed to identify the optimal conditions for epoxide production by examining the relationship between each variable and the response yield. The Box–Behnken design (BBD) method is one of the RSM

Table 1 Properties of polybenzimidazole supported Mo (*i.e.*, PBI·Mo) catalyst

Catalyst properties	PBI·Mo catalyst
BET surface area	18.44 m^2 g^{-1}
Pore volume	0.021986 cm^3 g^{-1}
Mo loading (mmol Mo per g resin)	0.825
Average pore diameter	21.595 Å
Average particle size	210–295 μm

Table 2 Experimental design variables and their coded level

Factors	Code	Levels		
		−1	0	1
FMR	*A*	2.5	6.25	10
Temperature (K)	*B*	333	343	353
Catalyst loading (mol%)	*C*	0.15	0.375	0.6
Time (min)	*D*	0	130	260

techniques used to examine the significant effect of process factors on the response.[24] Moreover, it examines how the interactions between the factors affect the response.[25] The experimental runs have been operated based on 4 independent variables including reaction feed molar ratio of 1,7-octadiene to TBHP, reaction temperature, catalyst loading, and reaction time which were labelled as *A*, *B*, *C*, and *D* respectively. Three levels for each variable have been coded as −1, 0, +1 as shown in Table 2. The yield of 1,2-epoxy-7-octene has been selected as the response for this study. The studies were finished in a random order to reduce the impact of unexplained inconsistency in the response.[26] Design Expert 13 software (Stat-Ease Inc., Minneapolis, MN, USA) was used to identify and operate the experimental design procedures. Twenty-nine runs were carried out randomly, and their responses were determined based on the outcomes of the experiment as shown in Table 3 (actual yield).[27]

Statistical analysis

To fit the experimental response with the independent variables, a model equation was developed.[28] The mathematical model was defined using the general quadratic model as shown in eqn (1).

$$Y = b_o + \sum_{i=1}^{n} b_i x_i + \sum_{i=1}^{n} b_{ii} x_i^2 + \sum_{i=1}^{n-1} \sum_{j>1}^{n} b_{ij} x_i x_j + \varepsilon \quad (1)$$

where Y is the predicted response (*i.e.*, yield of 1,2-epoxy-7-octene), b_o is the model coefficient constant, b_i, b_{ii}, b_{ij}, are coefficients for the intercept of linear, quadratic, interactive terms respectively, while x_i, x_j are independent variables ($i \neq j$), n is a number of independent variables and ε is the random error.

The adequacy of the predicted models was checked by several statistical validations including coefficient of correlation (R^2), adjusted coefficient of determination (R_{adj}^2) and the predicted coefficient of determination (R_{pred}^2). The statistical significance of the predicted models was analysed by ANOVA using Fisher's test, *i.e.*, *F*-test at a 95% confidence interval. The statistical significance of the results was presented by *p*-value, where the result is significant when the *p*-value is less than 0.05. Design Expert 13 software (Stat-Ease Inc., Minneapolis, MN, USA) was used to perform the initial

Table 3 Experimental design matrix with the actual and predicted yields

Run	FMR (*A*)	Temperature (K) (*B*)	Catalyst loading (mol%) (*C*)	Time (min) (*D*)	Actual yield (%)	Predicted yield (%)
1	6.25	353	0.15	130	49.88	47.48
2	6.25	343	0.375	130	52.29	52.29
3	10	343	0.375	0	0	−0.7667
4	10	333	0.375	130	38.61	40.59
5	6.25	343	0.375	130	52.29	52.29
6	6.25	343	0.6	0	0	2.41
7	6.25	333	0.15	130	37.23	38.01
8	6.25	333	0.375	260	51	47.82
9	6.25	333	0.375	0	0	−2.59
10	2.5	343	0.375	0	0	−1.60
11	6.25	343	0.375	130	52.29	52.29
12	2.5	343	0.375	260	48.38	47.48
13	2.5	353	0.375	130	44.32	44.10
14	6.25	353	0.375	0	0	3.09
15	6.25	343	0.15	260	53.46	52.81
16	10	343	0.15	130	41.2	42.33
17	6.25	343	0.15	0	0	−0.5350
18	10	343	0.6	130	54.47	52.70
19	10	353	0.375	130	53.57	53.06
20	6.25	353	0.375	260	61.23	63.73
21	6.25	343	0.6	260	57.82	60.11
22	6.25	333	0.6	130	41.07	41.81
23	10	343	0.375	260	61.28	61.21
24	2.5	343	0.6	130	41.38	40.16
25	2.5	343	0.15	130	38.62	40.30
26	6.25	353	0.6	130	56.38	53.93
27	6.25	343	0.375	130	52.29	52.29
28	6.25	343	0.375	130	52.29	52.29
29	2.5	333	0.375	130	32.72	34.99

Fig. 2 Reaction scheme for epoxidation of 1,7-octadiene with TBHP by PBI·Mo catalyst.

experimental design, model prediction, statistical analysis, and optimisation.

Batch epoxidation studies

A 0.25 L jacketed four-neck glass reactor was used for the batch epoxidation of 1,7-octadiene with TBHP as the oxidant in the presence of a polymer-supported Mo(VI) catalyst. The condenser, overhead stirrer, digital thermocouple, sampling point, and water bath were all included in the batch reactor's setup. Known quantities of 1,7-octadiene and TBHP were weighed out and added to the reactor vessel and stirrer speed was set at 400 rpm. The feed molar ratio (FMR) of 1,7-octadiene to TBHP of 2.5 : 1–10 : 1 was selected for charging the reactor. The temperature of the reaction mixture was allowed to reach the desired value, *i.e.*, 333–353 K, and was maintained throughout the batch experiment. When the reaction reached the correct temperature, a known quantity of catalyst (0.15–0.6 mol% Mo loading) was added. The reaction scheme for the epoxidation of 1,7-octadiene with TBHP is shown in Fig. 2.

A sample was collected after the catalyst was added and the time was noted as zero time, *i.e.*, t = 0. Subsequent samples were taken from the reaction mixture at specific time intervals and recorded. The samples collected were analysed using Shimadzu GC-2014 gas chromatography (GC).

Method of analysis

A specific quantity of internal standard (iso-octane) was added to samples and Shimadzu GC-2014 gas chromatography was used to analyse all the reactant and product compositions. The instrument was fitted with a flame ionisation detector (FID), auto-injector, and a 30 m long Econo-CapTM-5 (ECTM-5) capillary column. Helium was used as a carrier gas. The flow rate of carrier gas was 1 mL min^{-1}. The split ratio was 100 : 1 and an injection volume of 0.5 μL was selected. The temperature for both the injector and detector was 523 K. The oven temperature was maintained at 313 K for 4 minutes after the sample was injected and ramped from 313 K to 498 K at a rate of 20 °C per minute. Each sample takes ~13 min to be analysed by GC and the temperature was cooled back to 313 K before starting the next run.

Results and discussion

Development of regression model and adequacy checking

The predicted model was examined for adequacy in reporting any errors associated with the assumptions of normality. After performing the 29 experiments as shown in Table 3 and evaluating the yield of 1,2-epoxy-7-octene (reaction response) for each run, the response analysis using BBD has been applied. Design Expert software generated an equation of regression representing an empirical relationship between the response variable and the reaction parameters. By fitting the experimental results, the generic quadratic equation shown in eqn (1) was used to obtain a model of polynomial regression. The polynomial equation is shown in eqn (2).

$$Y = +52.29 + 3.64A + 5.40B + 2.56C + 27.76D + 0.8400AB + 2.63AC + 3.23AD + 0.6650BC + 2.56BD + 1.09CD - 5.27A^2 - 3.84B^2 - 3.15C^2 - 20.44D^2 \quad (2)$$

where Y represents the dependent variable (yield of epoxide). While A, B, C, and D represent the independent variables *i.e.*, feed molar ratio, temperature, catalyst loading, and time respectively. Further, AB, AC, AD, BC, BD, and CD represent the interaction between independent variables. Finally, A^2, B^2, C^2, and D^2 represent the excess of each independent variable.

The developed models have demonstrated the effect of each independent variable, variable interactions, and excess of each variable on the response. The positive sign of each variable coefficient represents the synergetic effect of the variable on the response. However, the negative sign represents the antagonistic effect on the response.[29]

It is clear from eqn (2), that the linear terms of feed molar ratio, temperature, catalyst loading, and time had positive coefficients, but their quadratic terms had negative coefficients. This would indicate that an increase in feed molar ratio, temperature, catalyst loading, and time to a certain extent, could increase the epoxide yield. However, a reduction in the epoxide yield could have occurred when applying too high a feed molar ratio, temperature, catalyst loading, and time.

ANOVA has been applied to examine the significance of the model parameters at a 95% confidence level. The significance of each parameter has been determined by F-test and p-value. The higher the value of the F-test and the smaller the p-value, the more significant the corresponding parameter.[30]

ANOVA has been used to validate the RSM model coefficient using the F-test and p-value. These values have been concluded as 159.75 and <0.0001, respectively as shown in Table 4 which proves that the developed quadratic model is statistically significant with a 95% confidence level. The determination coefficient values, R^2 and $R_{adj}{}^2$, which measure the reliability of the model fitting, have been calculated to be 0.9938 and 0.9876, respectively. The adequate precision is 38.74 which is desirable and ensures the model fitting to the experimental data.

The model performance has been observed using different techniques. A plot of the predicted *versus* experimental result of the yield of epoxide in Fig. 3 showed a high correlation and reasonable agreement. The good estimate for the response values from the model is concluded from the similarity between the predicted and actual experimental results as shown in Fig. 3. In addition, a plot of residual distribution *versus*

Table 4 Analysis of variance for response surface developed model

Source	Sum of squares	df	Mean square	*F*-Value	*p*-Value	Significance
Model	12 671.98	14	905.14	159.75	<0.0001	Significant
A-FMR	159.21	1	159.21	28.10	0.0001	Significant
B-Temperature	349.38	1	349.38	61.66	<0.0001	Very significant
C-Catalyst loading	78.69	1	78.69	13.89	0.0023	Significant
D-Time	9250.19	1	9250.19	1632.59	<0.0001	Very significant
AB	2.82	1	2.82	0.4981	0.4919	Not significant
AC	27.62	1	27.62	4.87	0.0445	Significant
AD	41.60	1	41.60	7.34	0.0169	Significant
BC	1.77	1	1.77	0.3122	0.5852	Not significant
BD	26.16	1	26.16	4.62	0.0496	Significant
CD	4.75	1	4.75	0.8388	0.3753	Not significant
A^2	180.06	1	180.06	31.78	<0.0001	Very significant
B^2	95.46	1	95.46	16.85	0.0011	Significant
C^2	64.31	1	64.31	11.35	0.0046	Significant
D^2	2710.34	1	2710.34	478.36	<0.0001	Very significant
Residual	79.32	14	5.67			
Lack of fit	79.32	10	7.93			
Pure error	0.0000	4	0.0000			
Cor total	12 751.31	28				

predicted response has been presented to check the fitting performance of the model as shown in Fig. 4. Residual value is defined as the difference between predicted and experimental values of the response variable. The plot confirms that the quadratic model adequately represents the experimental data as the distribution does not follow a specified trend with respect to the predicted values of the response variable. Moreover, the perturbation plot represents the effect of each variable on the reaction response as shown in Fig. 5. The curvature of the variables from the centre point indicates the significance of each variable which confirms the statistical results obtained from ANOVA as shown in Table 4. Sharp curvature of the independent variables, *e.g.*, time (*D*) and temperature (*B*) indicates their high significance as seen from the ANOVA results. It also represents the significance of feed molar ratio and catalyst loading. The plot indicates that time and temperature have progressively increasing effects on the yield of epoxide until reaching the central point and catalyst loading (*C*) is the least significant parameter.

Response surface plots analysis

3D response surface plots and their corresponding 2D contour plots were created for a model equation after constructing the regression model and evaluating the model adequacy. Different contour plot shapes represent differing levels of interaction between two variables. For example, an oval plot indicates strong interactions between the two specified variables, but a circular plot indicates otherwise.[31] 3D response surfaces help in understanding system behaviour. Additionally, it helps in identifying the reaction surface's characters.[32,33]

Effect of one factor at a time experiments on response (OFAT)

The 3D-surface and 2D-contour plots produced from the anticipated quadratic model have been used to investigate the effects of each independent process variable (feed molar ratio, temperature, catalyst loading, and time) and their interactions on reaction responses (epoxide yield), as shown in Fig. 6–9. The experiments have been carried out by varying one reaction parameter at a time while keeping other parameters constant at the following reaction conditions: feed molar ratio 6.25 : 1, reaction temperature 343 K, catalyst loading 0.375 (mol%), and time 130 min.

Effect of feed molar ratio (FMR). There is strong evidence that increasing the feed mole ratio (FMR) of the alkenes to

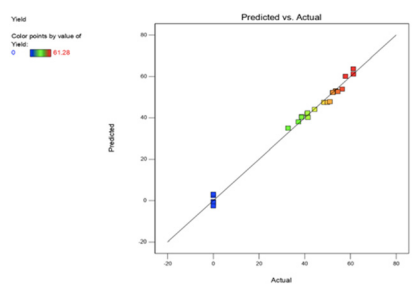

Fig. 3 Actual experimental data *versus* predicted model.

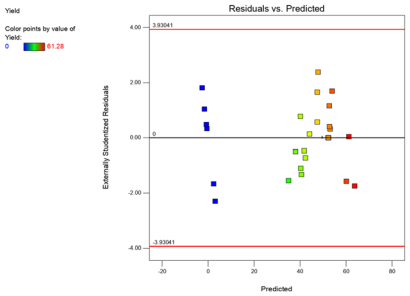

Fig. 4 Residual *versus* predicted response.

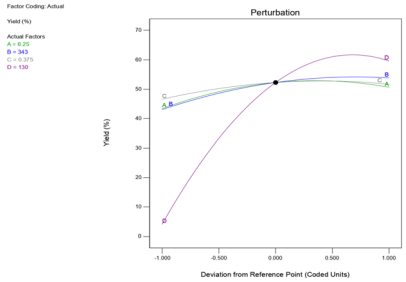

Fig. 5 The perturbation plot represents the effect of each variable on the reaction response.

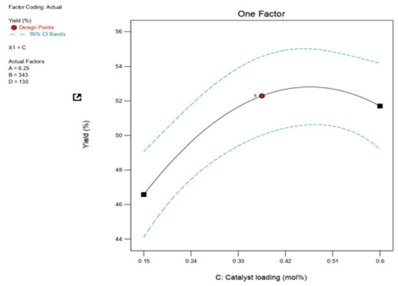

Fig. 8 The plot showing the effect of catalyst loading on the percentage yield.

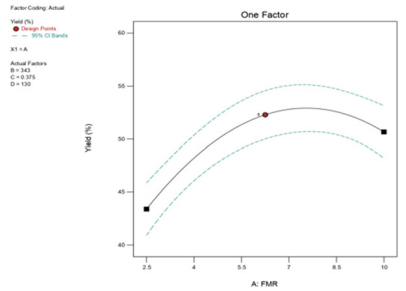

Fig. 6 The plot showing the effect of feed molar ratio on the percentage yield.

TBHP speeds up the production of the desired epoxides, as shown by the ANOVA results in Table 4. The impact of the feed molar ratio on epoxide yield was investigated by varying the feed molar ratio of alkene to TBHP between 2.5 : 1 and 10 : 1. Fig. 6 demonstrates that the rate of epoxide production increased steadily from 43.38% to 53% as the feed molar ratio increased from 2.5 : 1 to 7.6 : 1. However, when the FMR of an alkene to TBHP is raised from 7.85 : 1 to 10 : 1, epoxide formation is slowed. Fig. 6 suggests that alkene concentration affects the epoxidation of alkenes using a PBI catalyst.[9] Ambroziak *et al.*[34] mentioned that increasing the feed molar ratio lowers the TBHP concentration to such an extent that it slows down the conversion of TBHP into epoxide. A similar feed molar ratio effect was reported in my previous published results;[35] it has been demonstrated that there was no significant difference in the rate of epoxidation when the feed molar ratio of 1,5-hexadiene to TBHP was increased from 2.5 : 1 to 10 : 1.

Effect of reaction temperature. The rate of the reaction increases as the reaction temperature rises. As a result, a study was carried out to determine how reaction temperature affected epoxide yield. According to the findings of the ANOVA in Table 4, there is a very significant effect of reaction temperature on the process response. The influence of reaction temperature on epoxide yield has been investigated by varying temperatures over the range of 333 K to 353 K. Fig. 7 shows that when temperature increased from 333 K to 343 K, the epoxide yield increased consistently from 43.06% to 52.29% which is a directly proportional relationship between temperature and epoxide yield. It has been demonstrated that there was no significant difference in the yield of epoxide when the temperature was increased from 343 K to 353 K. However, at higher temperature values above 353 K, a progressive decline in yield was recorded. Mohammed *et al.* reported similar results for the epoxidation of 1-hexene with TBHP in the presence of PBI·Mo catalyst.[9]

Effect of catalyst loading. Catalyst loading is described in this study as a percentage of the mole ratio of Mo to TBHP. Due to a little variation in the measured value of Mo content acquired from several batches of produced catalysts, the active Mo component was chosen as the catalyst loading rather than the total mass of the catalyst. In this research, a single batch of the produced catalysts was used for batch investigations. The effect of catalyst loading for epoxidation of 1,7-octadiene with TBHP was investigated by conducting batch experiments using 0.15 mol% Mo, 0.375 mol% Mo, and 0.6 mol% Mo catalyst

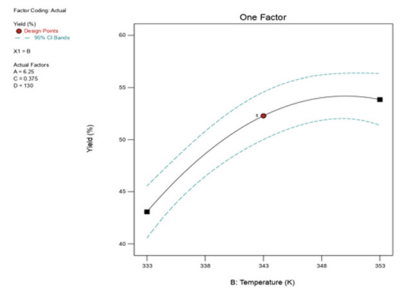

Fig. 7 The plot showing the effect of temperature on the percentage yield.

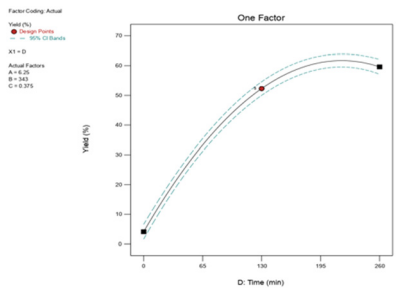

Fig. 9 The plot showing the effect of reaction time on the percentage yield.

loading. The results are presented in Fig. 8. Based on the ANOVA results presented in Table 4 catalyst loading parameter shows a very significant effect on the process response. As shown in Fig. 8, it can be observed that the yield of epoxide increased along with the increase in catalyst loading, from 46.58% to a maximum of 52.87% at 0.45 mol% Mo catalyst loading. It gradually declined once the catalyst loading was increased to 0.6 mol%, demonstrating that the optimum catalyst loading had been reached.

Effect of reaction time. In a catalytic reaction, reaction time is one of the most important variables. In this study, reaction time was calculated after the catalyst was added and the time was noted as zero time, *i.e.*, $t = 0$. Subsequent samples were taken from the reaction mixture at specific time intervals and recorded. Based on the ANOVA results presented in Table 4 the reaction time parameter shows a very significant effect on the process response. The yield of epoxide increased progressively as reaction time increased until it reached 60.4% in 218 min, as shown in Fig. 9, which illustrates a straight proportionality effect between reaction time and yield. Epoxide yield continued to decrease as reaction time was increased after 218 min. A similar phenomenon was reported for PBI·Mo catalysed epoxidation of 1-hexene and 4-vinyl-1-cyclohexene with TBHP, where an increase in reaction time from 0 to 260 min was directly proportional to corresponding epoxide yield.[9]

Effect of process variables and their interactions

Using ANOVA findings, 3D surface, and 2D contour plots, the interaction effect of each pair of reaction variables has been examined. When different levels of other variables are present, the interaction effect of specific process factors on epoxide yield produces different effects. The 3D-surface and 2D contour plots of the epoxide yield *versus* the interaction of two independent variables are displayed. The two remaining independent variables were kept constant at their centre points in each plot. When it comes to establishing precise forecasts about process optimization, 3D graphs have been instrumental.[36] According to ANOVA Table 4, all four reaction parameters are regarded as significant and have a significant impact on the process response at various levels of interaction. As a result, the interaction between process variables directly affects system optimization. Nandiwale and Bokade reported that if the contour plot of the response surface is circular, the interaction impact between a pair of variables would be insignificant. On the other hand, if the contour plot is elliptical, the interaction effect would be significant.[37] Therefore, the interactions were examined, which is important for a comprehensive optimization study, rather than just analysing a single variable (as in the conventional method).

Interactive effect of feed molar ratio and temperature. As depicted in Fig. 10 and the ANOVA Table 4, the interaction effect of feed molar ratio and reaction temperature has played significant roles in the yield of 1,2-epoxy-7-octene

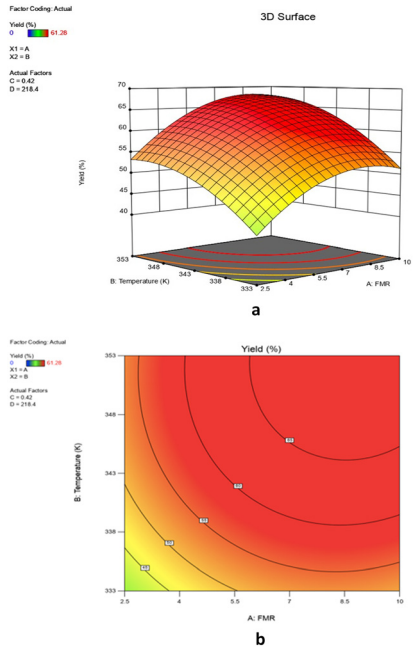

Fig. 10 (a) 3D response surface of the effect of feed molar ratio and temperature on percentage yield. (b) Contour plot of the effect of feed molar ratio and temperature on percentage yield.

while maintaining 0.42 mol% catalyst loading and reaction time 218 minutes. At a lower feed molar ratio (*e.g.*, at 2.5 : 1), an increase in the reaction temperature from 333 K to 348 K increases the epoxide yield from 40.6% to 53.4%. An increase in feed molar ratio 2.5 : 1 to 8.5 : 1 gave 53.4% and 68% yield of 1,2-epoxy-7-octene, respectively at 353 K. However, when the feed molar ratio of 1,7-octadiene to TBHP was beyond 8.5 : 1 there was no significant difference in the percentage yield of epoxidation (Fig. 10a). Increasing the feed molar ratio decreases the TBHP concentration to such an extent that it inhibits the conversion of TBHP into epoxide, which is the reason for the reduced epoxide yield. Furthermore, at a different level of interaction between feed molar ratio and temperature (*e.g.*, from 8.5 : 1 to 10 : 1 and 347–353 K), another noticeable effect was the steady drop in epoxide yield, an indication that the optimal conditions had been reached. This shows that variation in feed molar ratio had a negative effect on the yield of 1,2-epoxy-7-octene at higher values. As a result, the process response is significantly influenced by the relationship between feed molar ratio and temperature. A mutual interactive effect of the reaction variables on response is demonstrated by the elliptical shape of the 2D contour plot in Fig. 10b.

Interactive effect of feed molar ratio and catalyst loading. The overall epoxide yield has been significantly influenced by the interaction between the catalyst loading and feed molar ratio while reaction temperature and time have been kept at constant values of 348 K and 218 min, respectively. For example, Fig. 11 shows that at lower catalyst loading of 0.15 mol% Mo, only 48% of epoxide yield was recorded because of low 1,7-octadiene conversion at low catalyst loading. The

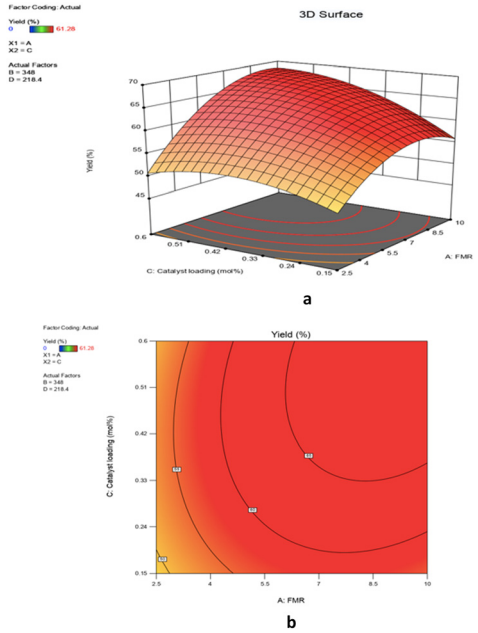

Fig. 11 (a) 3D response surface of the effect of feed molar ratio and catalyst loading on percentage yield. (b) Contour plot of the effect of feed molar ratio and catalyst loading on percentage yield.

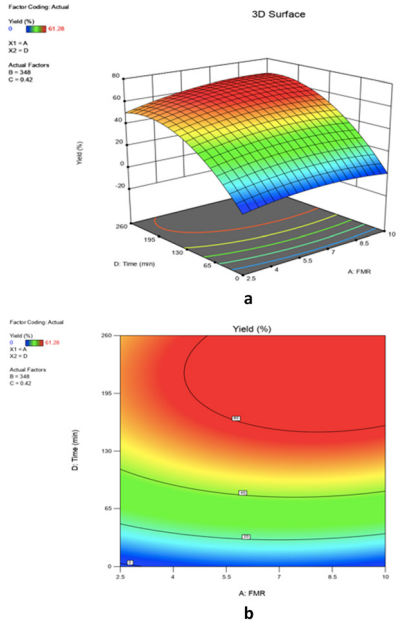

Fig. 12 (a) 3D response surface of the effect of feed molar ratio and time on percentage yield. (b) Contour plot of the effect of feed molar ratio and time on percentage yield.

epoxide yield increased steadily up to 67% as the feed molar ratio increased at moderate levels of catalyst loading from 0.15 mol% to 0.42 mol%. This phenomenon may be explained by an increase in the catalyst's surface area, which increases the surface area available for contact between the catalyst's active sites and the reactant 1,7-octadiene.[38] The increase in catalyst loading from 0.15 mol% Mo to 0.42 mol% enhances the epoxide yield from 48% to 53.1% for lower feed molar ratios (for example, at 2.5 : 1). An increase in feed molar ratio 2.5 : 1 to 8.5 : 1 gave 53% and 67.1% yield of 1,2-epoxy-7-octene, respectively at 0.42 mol% Mo. However, the percentage yield of epoxidation did not differ significantly when the feed molar ratio of 1,7-octadiene to TBHP was greater than 8.5 : 1 and the catalyst loading was greater than 0.42 mol% Mo (Fig. 11a). The contour plot in Fig. 11b with an elliptical shape demonstrated the significant and combined effect of the catalyst loading and feed molar ratio. The result has also supported a lower *p*-value (0.0445) of the interaction AC term. As seen in Fig. 11a, the yield of 1,2-epoxy-7-octene increases proportionally with catalyst loading at any designated value between 0.15 mol% and 0.42 mol%. A low *p*-value (0.0023) also provided support for this observation.

Interactive effect of feed molar ratio and time. Fig. 12 displays the interaction between the effects of reaction time and feed molar ratio on the yield of epoxide while keeping a catalyst loading of 0.42 mol% of Mo and a reaction temperature of 348 K. With lower feed molar ratios (for instance, at 2.5 : 1), the increase of reaction time from 0 min to 218 min improves the epoxide yield from 0% to 52.9%. Increasing the feed molar ratio from 2.5 : 1 to 8.5 : 1 resulted in yields of 1,2-epoxy-7-octene of 52.9% and 67.24%, respectively, after 218 minutes of reaction time. However, when the 1,7-octadiene to TBHP feed molar ratio was larger than 8.5 : 1 and the reaction time was greater than 218 minutes, the percentage yield of epoxidation did not change significantly (Fig. 12a). According to the 3D surface plot, the maximum epoxide yield (67.24%) was obtained at a reaction time of 218 minutes and a feed molar ratio of 8.5 : 1, showing that increasing the reaction time from 0 minutes to 218 minutes increases the yield of 1,2-epoxy-7-octene as shown in Fig. 12a. The results demonstrate a rise in epoxidation rate with increasing time. However, an increase in feed molar ratio of 1,7-octadiene to TBHP beyond 8.5 : 1 at 218 min of reaction time was unfavorable to the reactive system causing a marginal drop in epoxide yield from 67.24% to 66.66%. Response surface and contour plots of Fig. 12 clearly show that the yield of epoxide had a linear effect with increasing reaction time until the optimum condition was achieved. It can be concluded from the ANOVA Table 4 that the reaction time was found to be a highly influencing parameter on epoxide yield as evidenced by a low *p*-value (<0.0001).

Interactive effect of reaction temperature and reaction time. As shown in Fig. 13 and the ANOVA Table 4, the interaction effect of reaction duration and reaction temperature has significantly influenced the yield of 1,2-epoxy-7-octene while maintaining 0.42 mol% catalyst loading and a feed molar ratio of 1,7-octadiene to TBHP of 8.5 : 1. The 3-D surface plot revealed that the yield of epoxide was 67.07% at a reaction time of 218 minutes and temperature of 348 K, suggesting that raising the reaction temperature from 333 K to 348 K increases epoxide yield as shown in Fig. 13a. The yield of epoxidation did not change

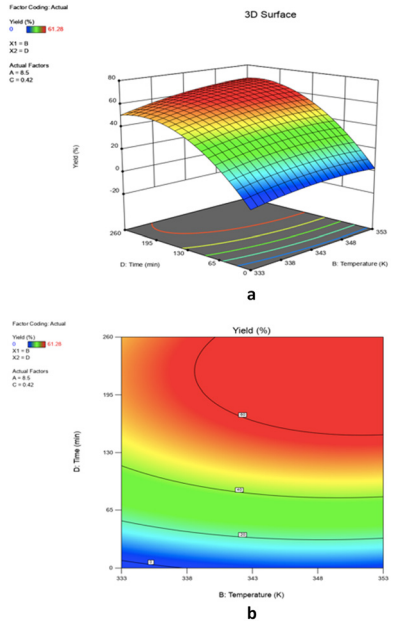

Fig. 13 (a) 3D response surface of the effect of reaction temperature and reaction time on percentage yield. (b) Contour plot of the effect of reaction temperature and reaction time on percentage yield.

considerably when the reaction temperature was raised above 348 K at 218 minutes. The yield of 1,2-epoxy-7-octene increased from 67.07% to 68.2% with a rise in reaction temperature from 348 K to 353 K. With an increase in reaction time from 218 minutes to 260 minutes at a reaction temperature of 348 K, the epoxide production slowly drops until it reaches 66.4%. In the presence of a PBI·Mo catalyst, Mohammed *et al.* and co-workers reported a similar outcome for the epoxidation of 1-hexene with TBHP.[9] When cyclohexene and limonene were oxidized with TBHP using PBI·Mo catalyst, at 353 and 343 K, a similar effect was observed.[39] The quality and stability of a product may also be impacted by chemical degradation or thermal decomposition losses at higher reaction temperatures.[40] A strong and combined effect of the catalyst loading and feed molar ratio on epoxide yield was demonstrated by the elliptical-shaped contour plot in Fig. 13b. The result has also supported a lower *p*-value (0.0496) of the interaction BD term. The reaction temperature has been demonstrated as a highly affecting parameter on percentage yield, as evidenced by the low *p*-value (<0.0001) in ANOVA Table 4.

Optimisation study of reaction variables

Due to regulatory regulations and rising intermediate manufacturing costs, there is an increasing quest for greener and more effective chemical synthesis methods. As a result, when investigating process optimum conditions and the interacting relationships between effective working variables, researchers are turning to RSM rather than more traditional optimization techniques. While using RSM, determining the best reaction parameters for a single answer is rather straightforward, while optimising many responses is more difficult.[38] An optimisation process of the epoxidation reaction has been carried out to define the optimum values for the independent variables affecting the dependent response variable. Design Expert software has been used to develop the numerical optimisation step by combining the desirability of each independent variable into a single value and then searching for optimum values for the response goals. Accordingly, to determine the optimum conditions of the independent variables, a set of targets must be defined on the software to guide the optimisation process.[30] Table 5 shows the optimization targets for this study, the values have been set to maximize the process productivity.

Table 5 Optimisation criteria used to predict optimum condition for the yield of 1.2-epoxy-7-octene synthesis

			Limits	
Factor	Code	Goal	Lower	Upper
FMR	*A*	In range	2.5	10
Temperature (K)	*B*	Minimise	333	353
Catalyst loading (mol%)	*C*	In range	0.15	0.6
Time (min)	*D*	Minimise	0	260
Epoxide yield	*Y*	Maximise	30	68

The reaction temperature and time have both been targeted to minimal values to minimise production cost at a maximum economic benefit, while the dependent response variable, which is the yield of 1,2-epoxy-7-octene, has been set to be maximised to obtain the maximum yield. No specific target for catalyst loading has been established due to the catalyst's stability and efficiency at optimal conditions. The numerical optimisation technique concluded that the maximum yield that can be reached is 66.22% at a feed molar ratio of 7.97 : 1, reaction temperature 347 K, 0.417 mol% catalyst loading, and reaction time of 218 min.

Optimum conditions validation

The main aim of this research is to identify optimal conditions for epoxide formation using the response surface methodology (RSM) technique. As a result, after finishing the five experiments which constitute the central point of the experimental design, the median value was taken to finish the experimental design and it has been proved statistically significant. To validate the optimal response values of the predicted quadratic equation, experiments have been performed at optimum conditions *i.e.*, feed molar ratio of 7.97 : 1, reaction temperature 347 K, 0.417 mol% catalyst loading, and reaction time of 218 min. The experimental results showed a similar response value to the predicted optimal response of 64.97% with a relative error of 1.92%. The relative error can be affected by the temperature variation of the reaction.

Conclusions

The polymer-supported Mo(VI) (PBI·Mo complex) has been prepared and characterized. Using TBHP as an oxidant, the

performance of the catalyst was evaluated for the epoxidation of 1,7-octadiene in a jacketed stirred batch reactor. PBI·Mo catalyst has been proven to be active for batch reactions. Reaction variables and operating conditions of the reaction have been optimised. A quadratic polynomial model has been developed demonstrating the yield of 1,2-epoxy-7-octene in four independent variables. Batch epoxidation experiments were carried out to analyse the effect of temperature, the molar ratio of reactants, and catalyst loading on the yield of 1,2-epoxy-7-octene. The optimum conditions observed for the maximum yield of 1,2-epoxy-7 octene are a 7.97 : 1 molar feed ratio of alkene to TBHP, 347 K reaction temperature, 218 min reaction time, and 0.417 mol% catalyst loading. The optimisation result has been validated experimentally resulting in an epoxide yield of 64.97%, which shows the adequacy of the predicted optimum conditions with a 1.92% relative error from the experimental results. This study demonstrates that polymer-supported Mo(VI) (PBI·Mo complex) could be used as an effective catalyst for a greener and more efficient epoxidation of 1,7-octaadiene with *tert*-butyl hydroperoxide (TBHP) as an oxidising reagent.

Author contributions

M. M. R. B. – methodology, software, validation, visualization, formal analysis, data curation, writing – original draft preparation; B. S. – conceptualization, writing – review and editing, formal analysis, data curation, resources, supervision, and project administration.

Conflicts of interest

There are no conflicts to declare.

References

1 R. Mbeleck, M. L. Mohammed, K. Ambroziak, D. C. Sherrington and B. Saha, *Catal. Today*, 2015, **256**, 287–293.
2 M. L. Mohammed and B. Saha, *Energies*, 2022, **15**, 1–15.
3 R. Mbeleck, K. Ambroziak, B. Saha and D. C. Sherrington, *React. Funct. Polym.*, 2007, **67**, 1448–1457.
4 S. E. Schaus, B. D. Brandes, J. F. Larrow, M. Tokunaga, K. B. Hansen, A. E. Gould, M. E. Furrow and E. N. Jacobsen, *J. Am. Chem. Soc.*, 2002, **124**, 1307–1315.
5 G. Grivani, S. Tangestaninejad, M. H. Habibi and V. Mirkhani, *Catal. Commun.*, 2005, **6**, 375–378.
6 G. Grivani, S. Tangestaninejad, M. H. Habibi, V. Mirkhani and M. Moghadam, *Appl. Catal., A*, 2006, **299**, 131–136.
7 E. Santacesaria, R. Tesser, M. D. Serio, R. Turco, V. Russo and D. Verde, *Chem. Eng. J.*, 2011, **173**, 198–209.
8 The Many Uses and Hazards of Peracetic Acid, **https://synergist.aiha.org/201612-peracetic-acid-uses-and-hazards**, (accessed August 2023).
9 M. L. Mohammed, D. Patel, R. Mbeleck, D. Niyogi, D. C. Sherrington and B. Saha, *Appl. Catal., A*, 2013, **466**, 142–152.
10 J. Kollar, Epoxidation Process, *US Pat.*, US53617966A, 1967.
11 M. Salavati-Niasari, E. Esmaeili, H. Seyghalkar and M. Bazarganipour, *Inorg. Chim. Acta*, 2011, **375**, 11–19.
12 Y. Shen, P. Jiang, J. Zhang, G. Bian, P. Zhang, Y. Dong and W. Zhang, *Mol. Catal.*, 2017, **433**, 212–223.
13 C. Bisio, A. Gallo, R. Psaro, C. Tiozzo, M. Guidotti and F. Carniato, *Appl. Catal., A*, 2019, **581**, 133–142.
14 L. Cai, C. Chen, W. Wang, X. Gao, X. Kuang, Y. Jiang, L. Li and G. Wu, *Ind. Eng. Chem. Res.*, 2020, 191–200.
15 Z. Wu, Z. He, D. Zhou, Y. Yang, X. Lu and Q. Xia, *Mater. Lett.*, 2020, 128549.
16 W. Lueangchaichaweng, B. Singh, D. Mandelli, W. A. Carvalho, S. Fiorilli and P. P. Pescarmona, *Appl. Catal., A*, 2019, **571**, 180–187.
17 E. Mikolajska, V. Calvino-Casilda and M. A. Bañares, *Appl. Catal., A*, 2012, 164–171.
18 V. B. Borugadda and V. V. Goud, *Energy Procedia*, 2014, **54**, 75–84.
19 C. Peng, X. H. Lu, X. T. Ma, Y. Shen, C. C. Wei, J. He, D. Zhou and Q. H. Xia, *J. Mol. Catal. A: Chem.*, 2016, **423**, 393–399.
20 K. Otake, S. I. Ahn, J. Knapp, J. T. Hupp, J. M. Notestein and O. K. Farha, *Inorg. Chem.*, 2021, **60**, 2457–2463.
21 M. L. Mohammed and B. Saha, in *Ion Exchange and Solvent Extraction*, ed. A. K. SenGupta, CRC Press, Boca Raton, 2016, p. 33.
22 L. Paglia, V. Genova, M. P. Bracciale, C. Bartili, F. Marra, M. Natali and G. Pulci, *J. Therm. Anal. Calorim.*, 2020, **142**, 2149–2161.
23 J. Yuan, J. Huang, G. Wu, J. Tong, G. Xie, J. Duan and M. Qin, *Ind. Crops Prod.*, 2015, **74**, 192–199.
24 O. Aboelazayem, M. Gadalla and B. Saha, *Renewable Energy*, 2018, **124**, 144–154.
25 M. Khajeh, *J. Food Compos. Anal.*, 2009, **22**, 343–346.
26 H. Jaliliannosrati, N. A. S. Amin and A. Talebian-Kiakalaieh, *Bioresour. Technol.*, 2013, **136**, 565–573.
27 V. Onyenkeadi, O. Aboelazayem and B. Saha, *Catal. Today*, 2020, **346**, 10–22.
28 O. Aboelazayem, N. S. El-Gendy, A. A. Abdel-Rehim and F. Ashour, *Energy*, 2018, **157**, 843–852.
29 N. S. El-Gendy, A. A. S. A. El-Gharabawy, S. S. A. Amr and F. H. Ashour, *Int. J. ChemTech Res.*, 2015, **8**, 385–398.
30 N. S. El-Gendy, S. F. Deriase and A. Hamdy, *Energy Sources, Part A*, 2014, **36**, 623–637.
31 D. W. Lee, N. Marasini, B. K. Poudel, J. H. Kim, H. J. Cho, B. K. Moon, H. G. Choi, C. S. Yong and J. O. Kim, *J. Microencapsulation*, 2014, **31**, 31–40.
32 X. Long, L. Cai and W. Li, *Constr. Build. Mater.*, 2019, **197**, 406–420.
33 H. Mohammadifard and M. C. Amiri, *J. Water Environ. Nanotechnol.*, 2018, **3**, 141–149.
34 K. Ambroziak, R. Mbeleck, B. Saha and D. C. Sherrington, *Int. J. Chem. React. Eng.*, 2010, **8**, 1–13.
35 M. M. R. Bhuiyan, M. L. Mohammed and B. Saha, *Reactions*, 2022, **3**, 537–552.

36 M. Bahrami, M. J. Amiri and F. Bagheri, *J. Environ. Chem. Eng.*, 2019, **7**, 700–793.
37 K. Y. Nandiwale and V. V. Bokade, *Ind. Eng. Chem. Res.*, 2014, **53**, 18690–18698.
38 B. Olaniyan and B. Saha, *Energies*, 2020, **13**, 741.
39 K. Ambroziak, R. Mbeleck, Y. He, B. Saha and D. C. Sherrington, *Ind. Eng. Chem. Res.*, 2009, **48**, 3293–3302.
40 J. Peng, S. Wang, H. Yang, B. Ban, Z. Wei, L. Wang and B. Lei, *Fuel*, 2018, **224**, 481–488.